2011 Mar 3 at IPMU

Active galaxies observed with integral field spectroscopy

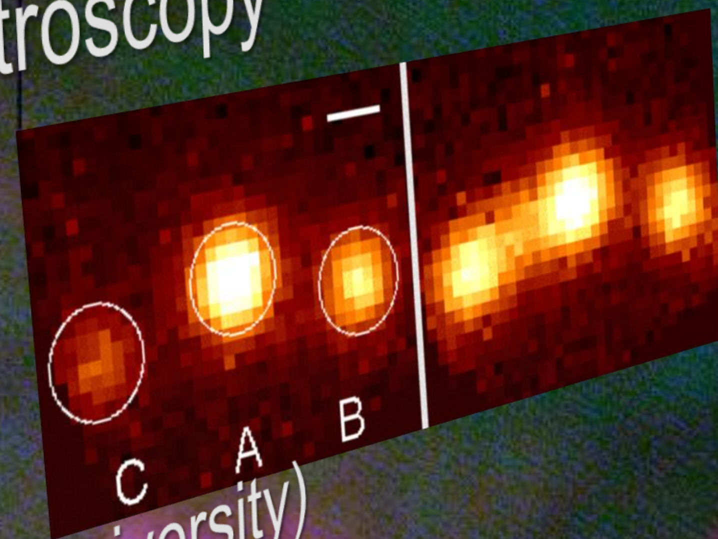

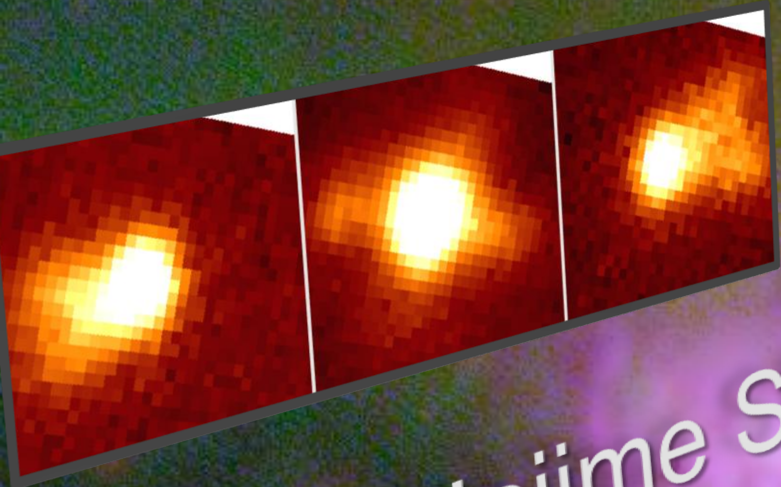

Hajime SUGAI (Kyoto University)

Today's talk

Instrumentation

Kyoto 3DII

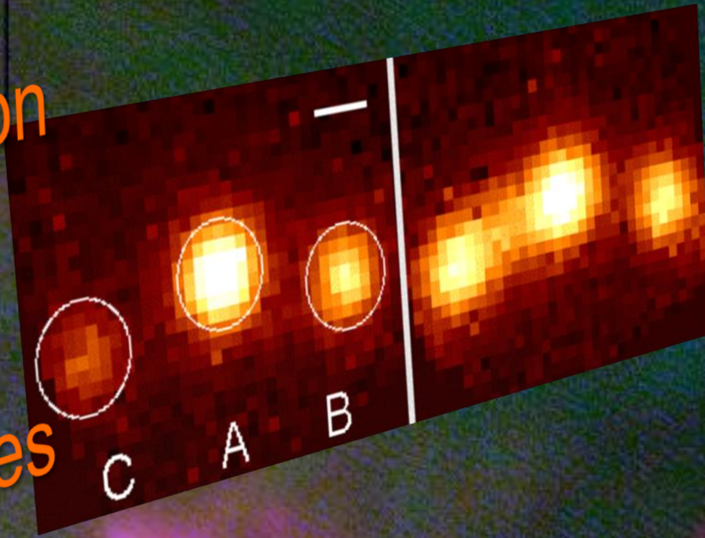

Active galaxies

young AGN wind

gravitationally lensed quasar

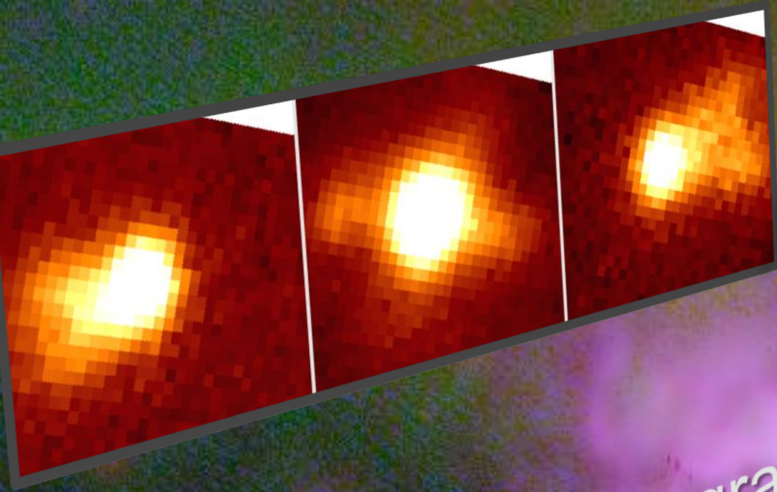

Strengths of Subaru Telescope

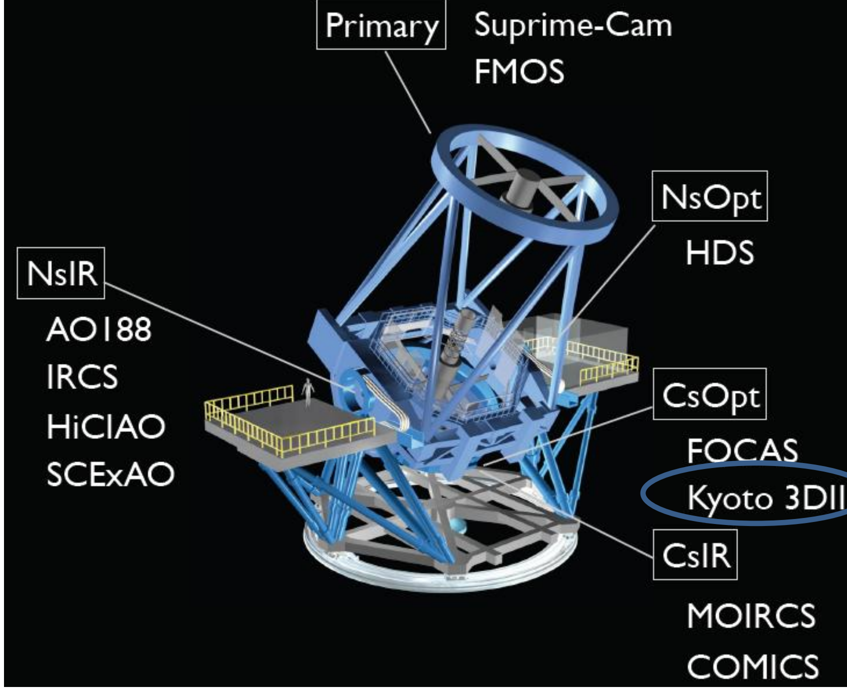

Figure: Iwata, 2011, Subaru Future Instr. WS

Large Field of View

e.g., Suprime Cam

(Hyper Suprime Cam, Prime Focus Spectrograph)

Platescale (arcsec mm-1) $\propto$ 1/f → prime focus

(rigid tel. structure)

Excellent Image Quality

e.g., today's talk

mirror surface, dome shape, rigid structure, tel. tracking

What is Kyoto 3DII???

Answer: PI instrument of Subaru

PI instruments	If you want to use the PI instruments such as CIAO or Kyoto3DII, please make contact with the instrument team in advance. The contact address for CIAO is *ishii@naoj.org* , and for Kyoto3DII is *sugai@kusastro.kyoto-u.ac.jp*

http://subarutelescope.org/Observing/Proposals/Submit/call.html

What is Kyoto 3DII??

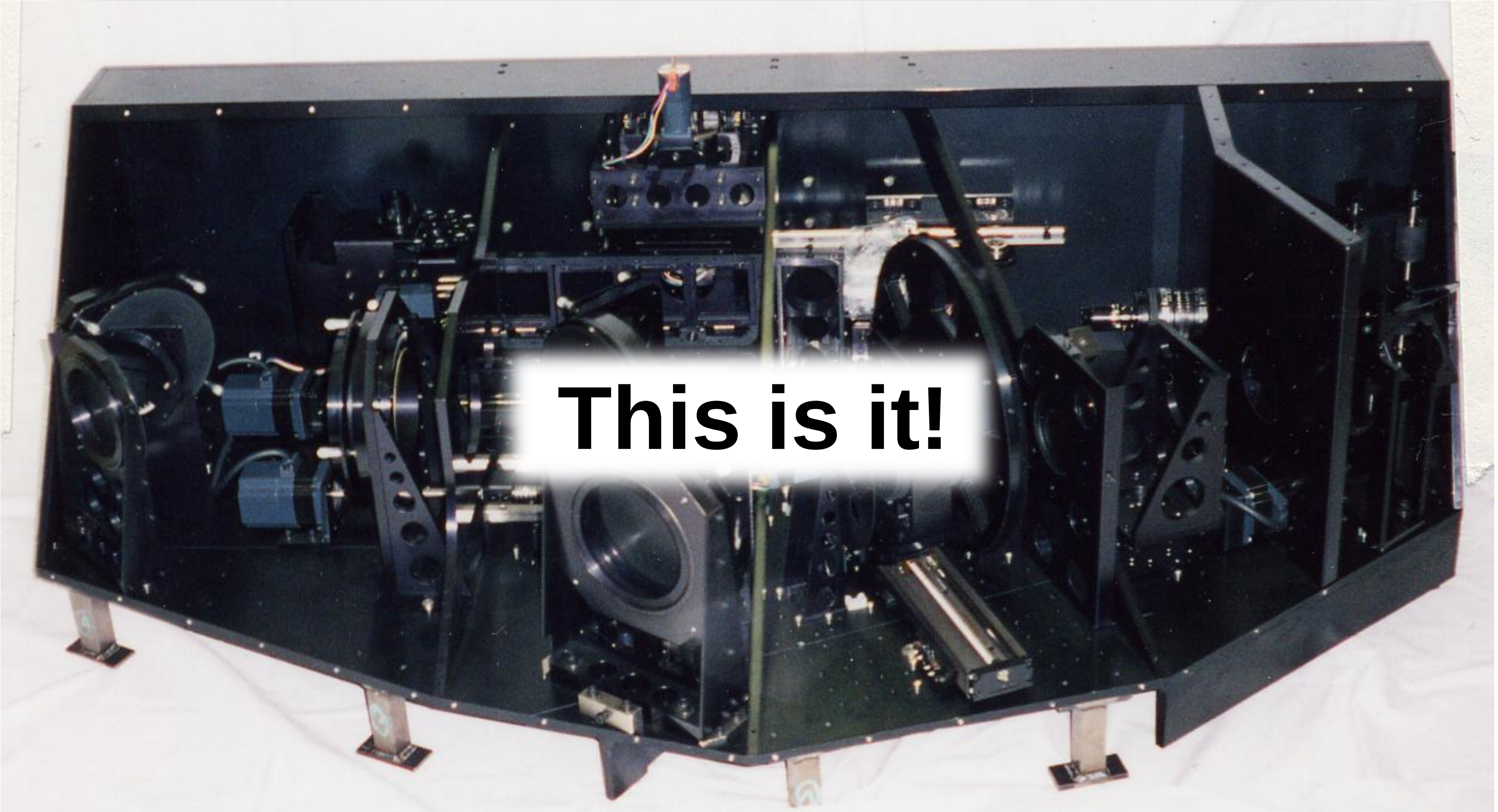

1.5m

150kg

What is Kyoto 3DII?

Multi-mode Optical (360-900nm) Spectrograph at Cassegrain

i) Lenslet-type Integral Field Spectrograph (IFS)
ii) Fabry-Perot
iii) Slit Spectrograph
iv) Filter Imaging

in this talk

(Sugai et al., 2010, PASP, 122, 103)
cf. Nasmyth focus in case of 3DII + AO188

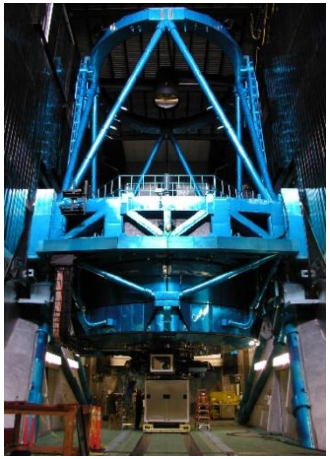

on Subaru Cass.
(2002 Aug)

Table 1: Observing Parameters

Observational mode	On Subaru (8.2 m, F/12.2)
Fabry-Perot	$0''.056$ pixel^{-1} [a] Field of view $1'.9 \times 1'.9$[b] (Velocity shift Δv (km s^{-1}) $= 980 \times (\theta')^2$) R $\equiv \lambda/\Delta\lambda \sim 400$ and 7000 (400 – 700 nm)[c]
Integral field spectrograph with a lenslet array (+ 34× enlarger)	$0''.096$ lens^{-1} Field of view $3''.6 \times 2''.8$(object) $+3''.6 \times 0''.6$(sky) R $\simeq 1200$ (360 – 900 nm)[d,e]
Long slit	Width $0''.12$, $0''.19$, $0''.56$ or Width $0''.17$, $0''.62$, $2''.1$ Length $1'.5$ R $\simeq 1200$ for $0''.12$ slit[d]
Narrow-band imaging	$0''.056$ pixel^{-1} Field of view $1'.9 \times 1'.9$

BASICS

standard slit spectrograph

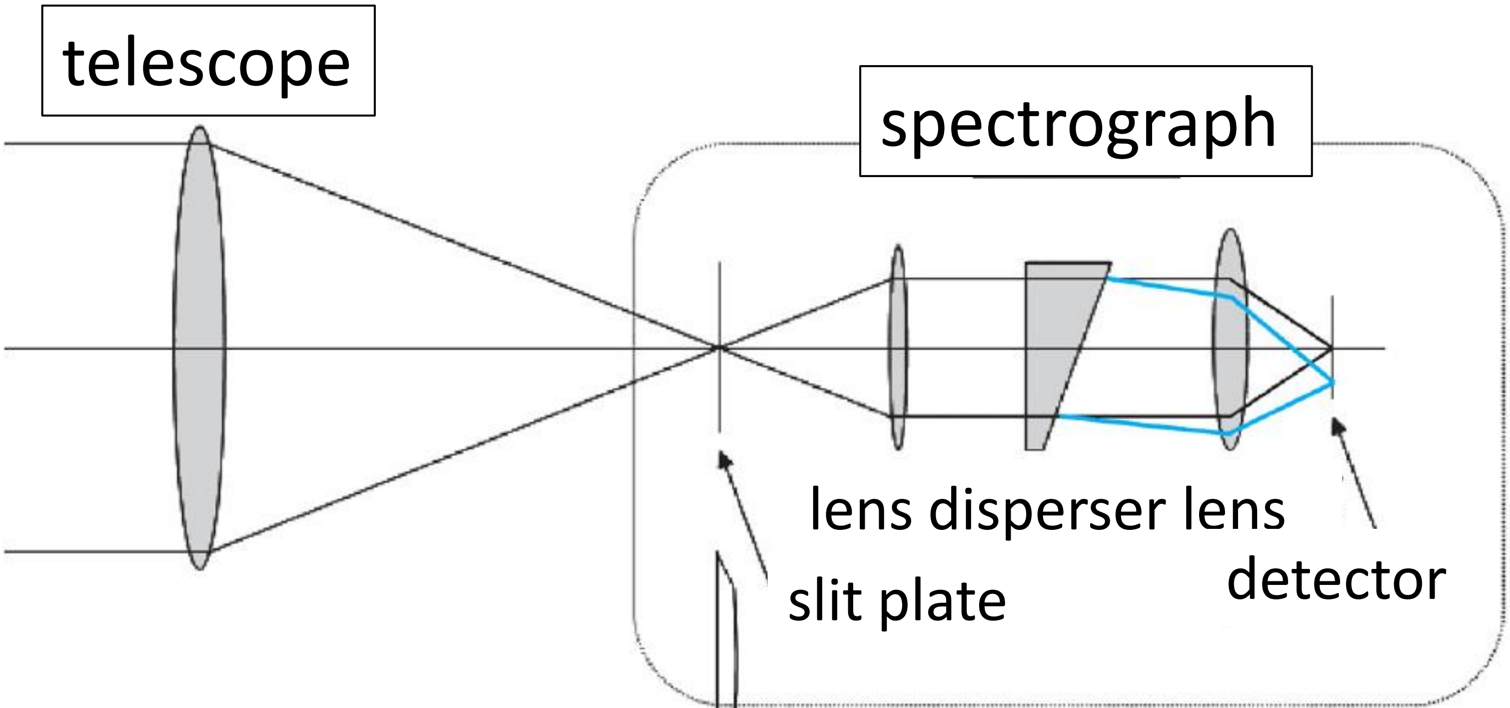

Slit plate viewed from telescope side.
Target image is produced on the plate,
and only light coming through the slit
(one spatial dimension) can be observed.

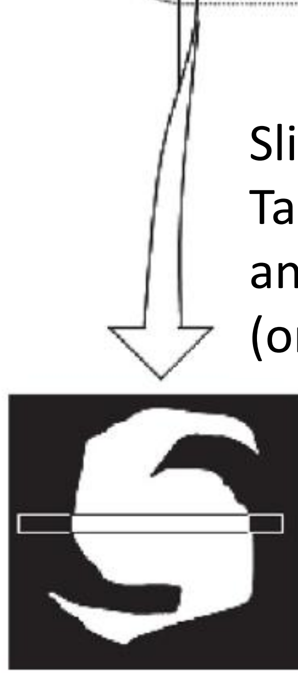

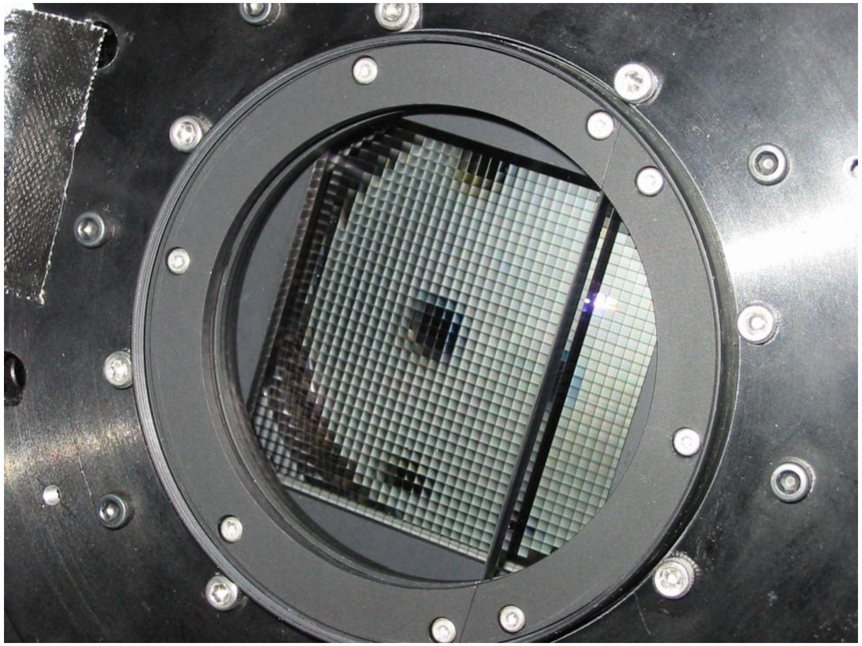

Now, difference for lenslet-type IFS from standard slit spectrograph

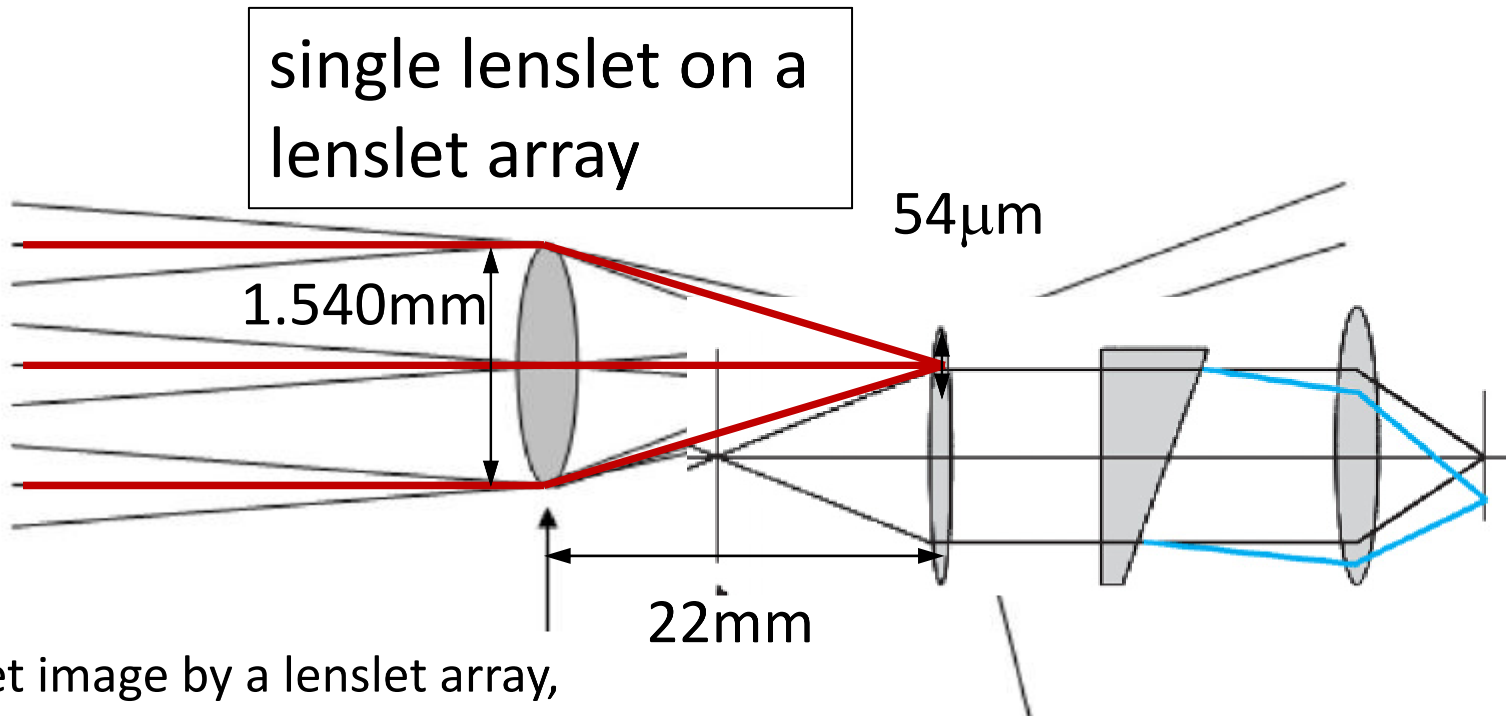

Dividing target image by a lenslet array, at surface of which the target image is produced by telescope (and enlarger).

Pupil image position.
Match this position with
the entrance of spectrograph
("slit position of ordinary spectrograph").

How do lenslet-type IFS data look like?

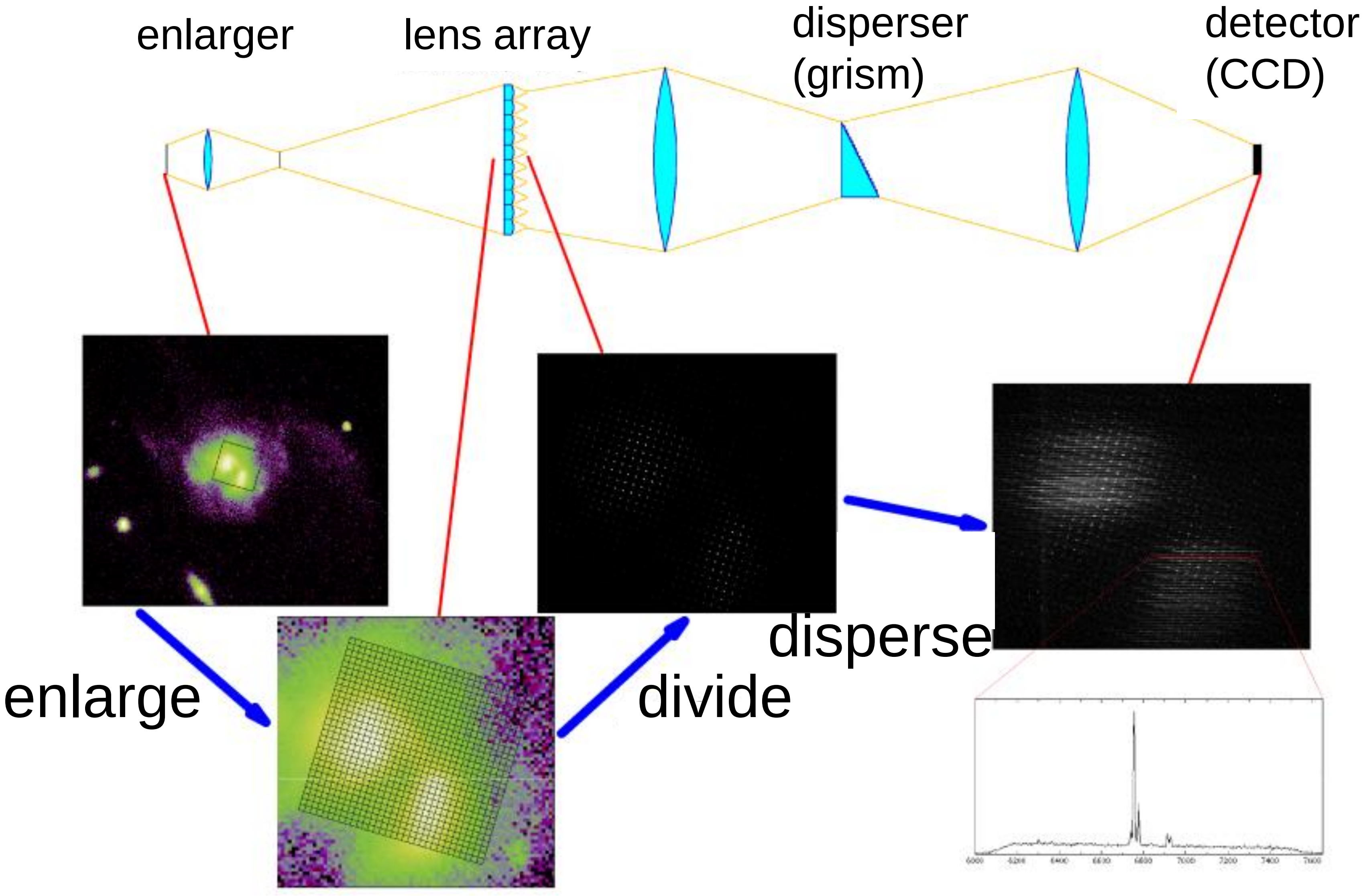

Figure: Takashi Hattori

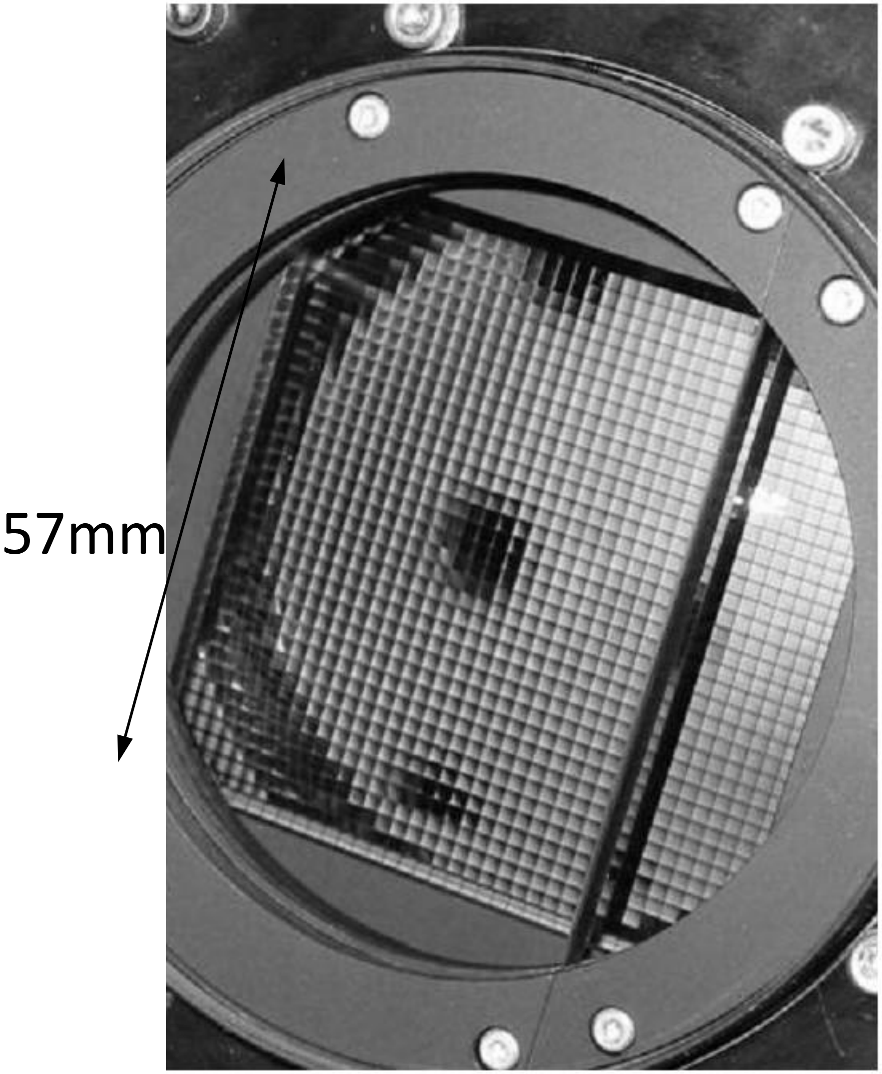

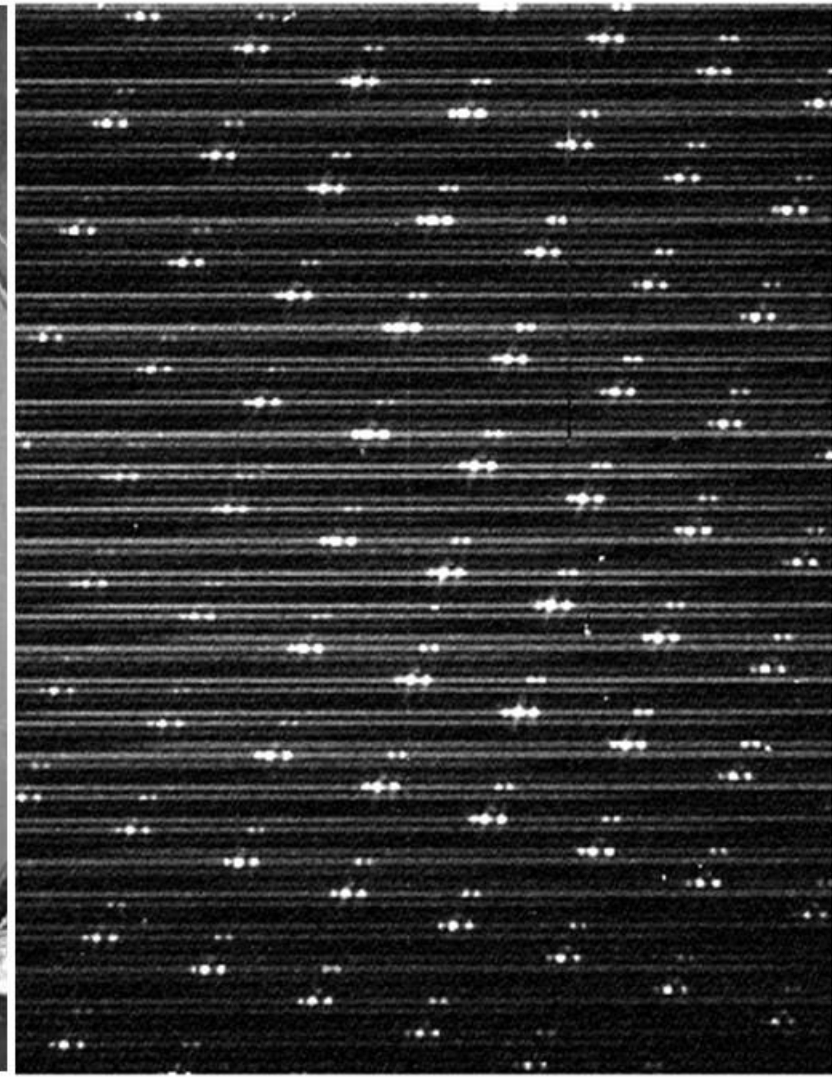

Crossed cylindrical lenslet array
--- divides an enlarged target image
into spatial elements

Example of actually obtained target spectra.
Only a small part of detector is shown.

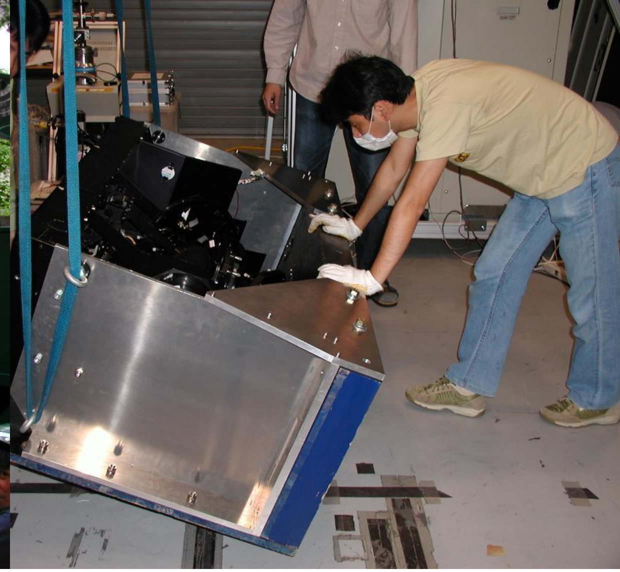

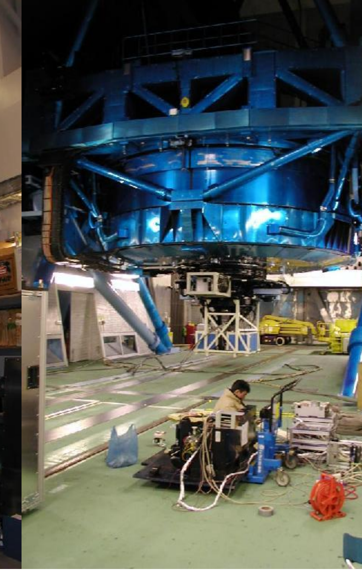

Procedures taken as a PI instrument before test obs. at Subaru

(now it is much more simplified at least for small PI projects)

Test of Connection between 3DII and its container for Subaru (at NAOJ, Tokyo)
Test of Thermal Control of 3DII by connecting with “dummy” container (at NAOJ, Tokyo)
Test observations at 1.5m “Subaru simulator” telescope (at NAOJ, Tokyo)

Reviewed by Technical committee
Reviewed by Science committee
Mechanical test at “Subaru Cassegrain” simulator (at Hilo, Hawaii)
Test observations at University of Hawaii 88-inch telescope (at Mauna Kea, Hawaii)
Test observations at Subaru telescope (at Mauna Kea, Hawaii)

Examples of high resolution observations

1. “Subarcsecond structure and velocity field of optical line-emitting gas in NGC 1052”

   H. Sugai, T. Hattori, A. Kawai, S. Ozaki, G. Kosugi, H. Ohtani,
   T. Hayashi, T. Ishigaki, M. Ishii, M. Sasaki, N. Takeyama,
   M. Yutani, T. Usuda, S. S. Hayashi, K. Namikawa, 2005, ApJ, 629, 131.

2. “Integral field spectroscopy of the quadruply lensed quasar 1RXS J1131-1231: new light on lens substructures”

   H. Sugai, A. Kawai, A. Shimono, T. Hattori, G. Kosugi,
   N. Kashikawa, K. T. Inoue, M. Chiba, 2007, ApJ, 660, 1016.

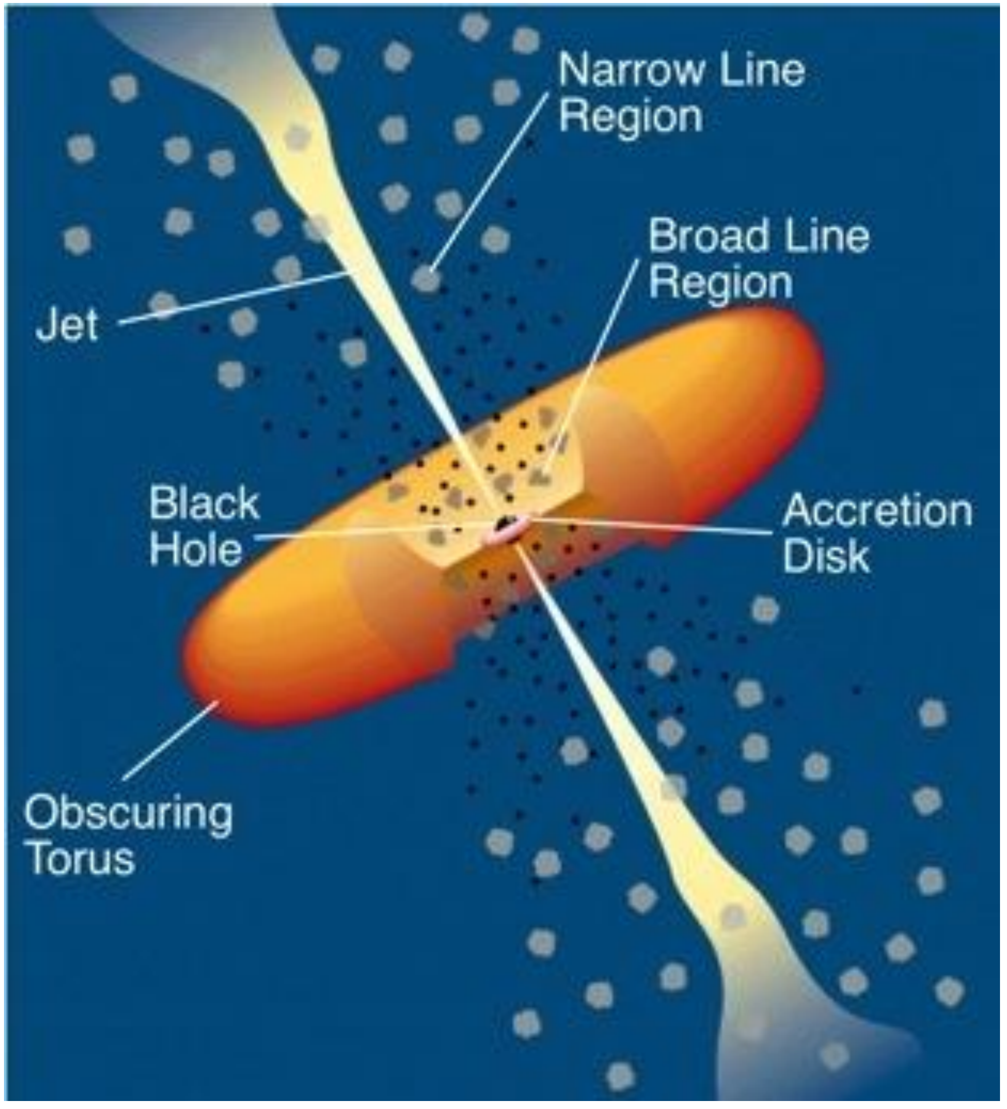

Urry & Padovani (1995)

Subarcsecond structure and velocity field of optical line-emitting gas in NGC 1052

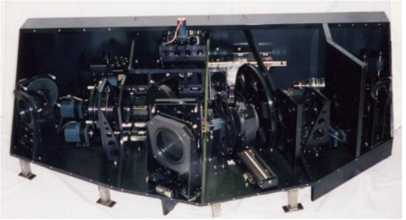

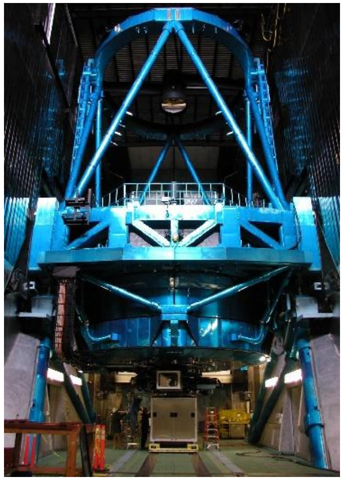

1. Background
2. Abstract
3. Observations
4. Results
   4-1. Three components
   4-2. Structures in bipolar outflow
   4-3. Bipolar outflow & radio jets
5. Summary

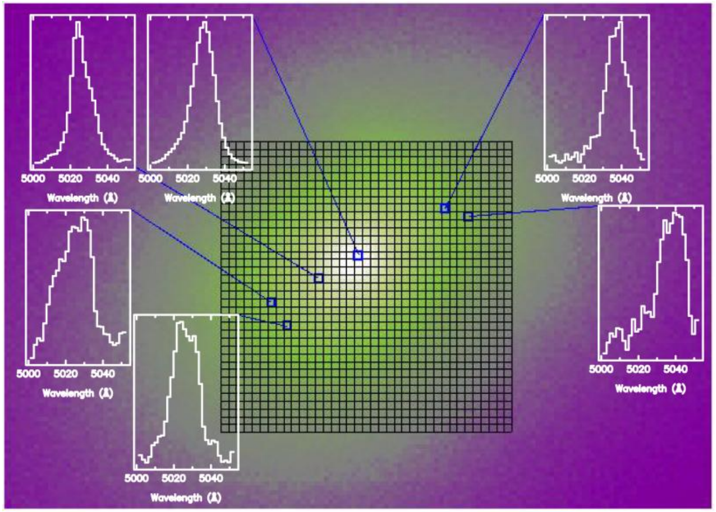

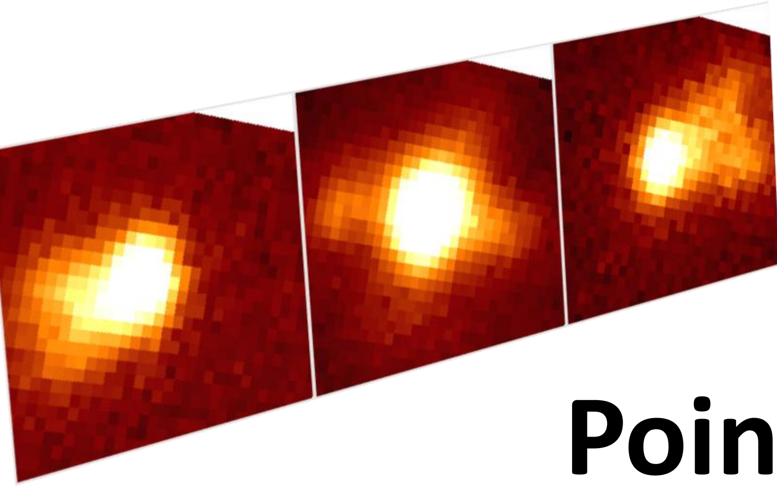

Point: NGC 1052

resolve spatial and kinematic structures
within the **AGN outflow**

Background: NGC 1052

pure AGN outflow

complication for AGN-driven outflows: they sometimes coexist with starburst-driven outflows（Veilleux et al. 2005）

---no evidence of starbursts in NGC 1052

young activities

similar to Gigahertz-Peaked-Spectrum or Compact-Steep-Spectrum sources

the entire radio source contained within the host galaxy.

a convex radio spectrum peaked at 10 GHz.

-→ young jets, propagating through, and perhaps interacting with, a rich inner galactic medium

Observations

Kyoto 3DII IFS mode (37x37 lenslet array)
+ Subaru 8.2m telescope

4200-5200A(a 60min exposure, R=1200)
Spatial sampling = 0”.096 lenslet^{-1}
→ Field of View~3”.6 x 2”.8
Spatial resolution = 0”.4

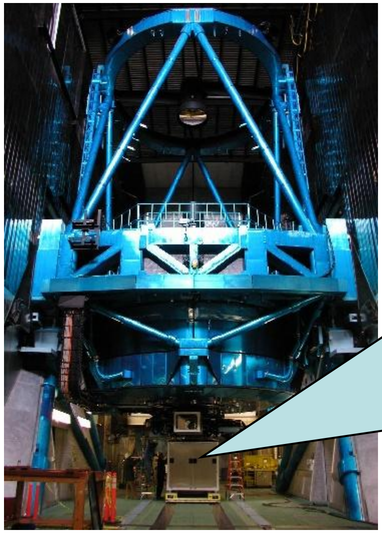

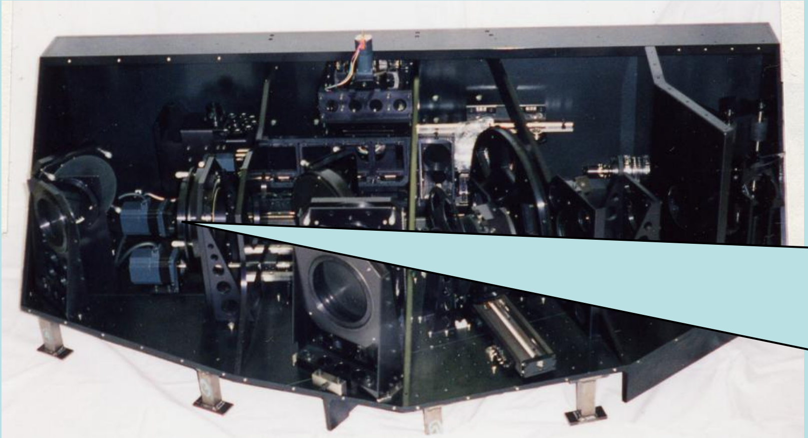

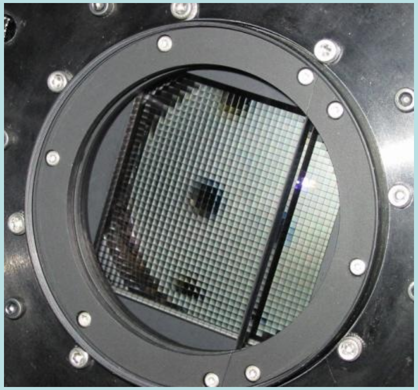

Spectrum of central region of NGC 1052

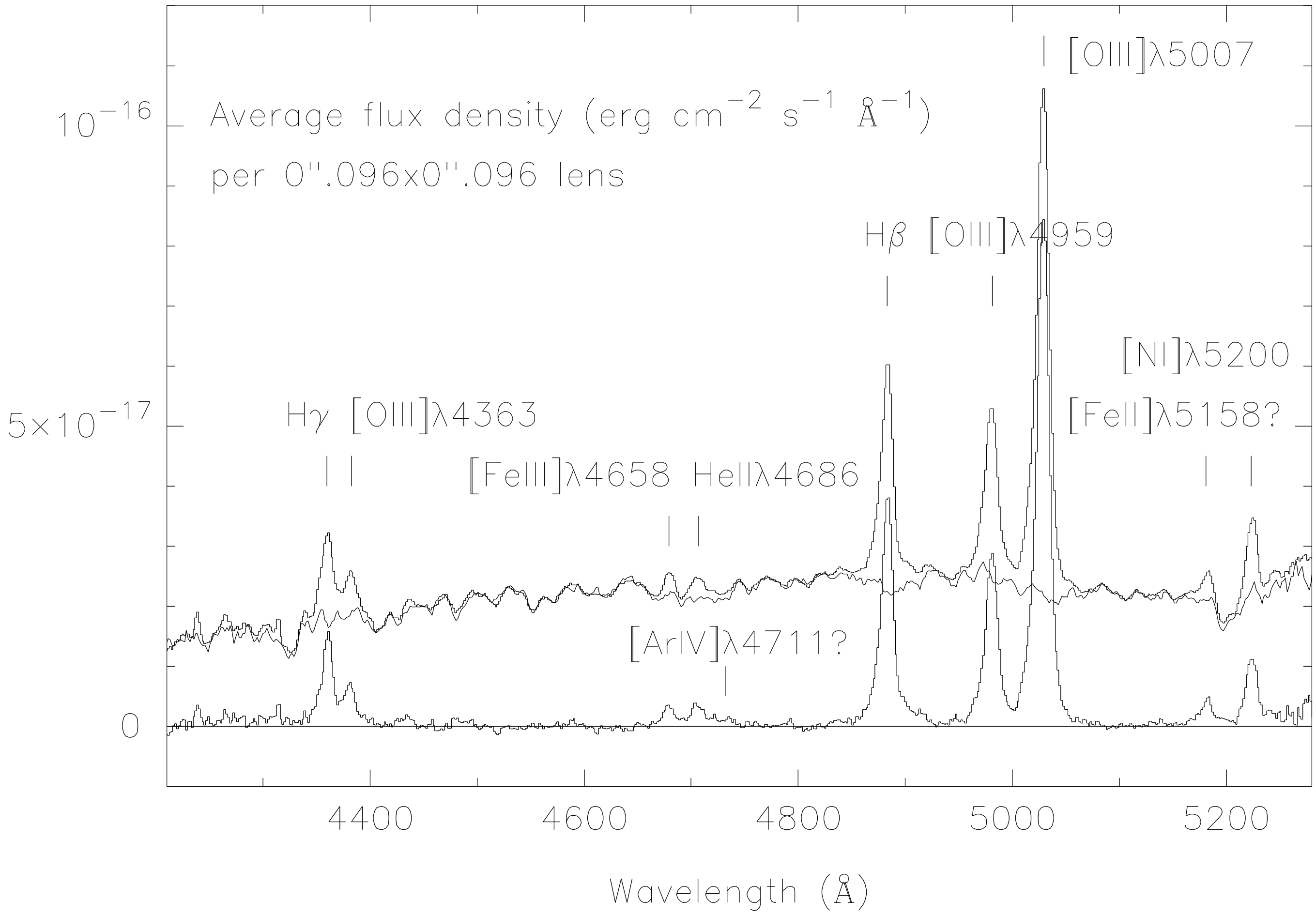

Spectrum of the central 0”.4 x 0”.4 region of NGC 1052. The spectrum of the central region of NGC 821 is also shown, after matching redshift and flux between the two galaxies. The bottom spectrum is the continuum-subtracted one of NGC 1052.

Velocity channel maps of [OIII]λ5007 line

0".4 resolution in
1-hr exposure

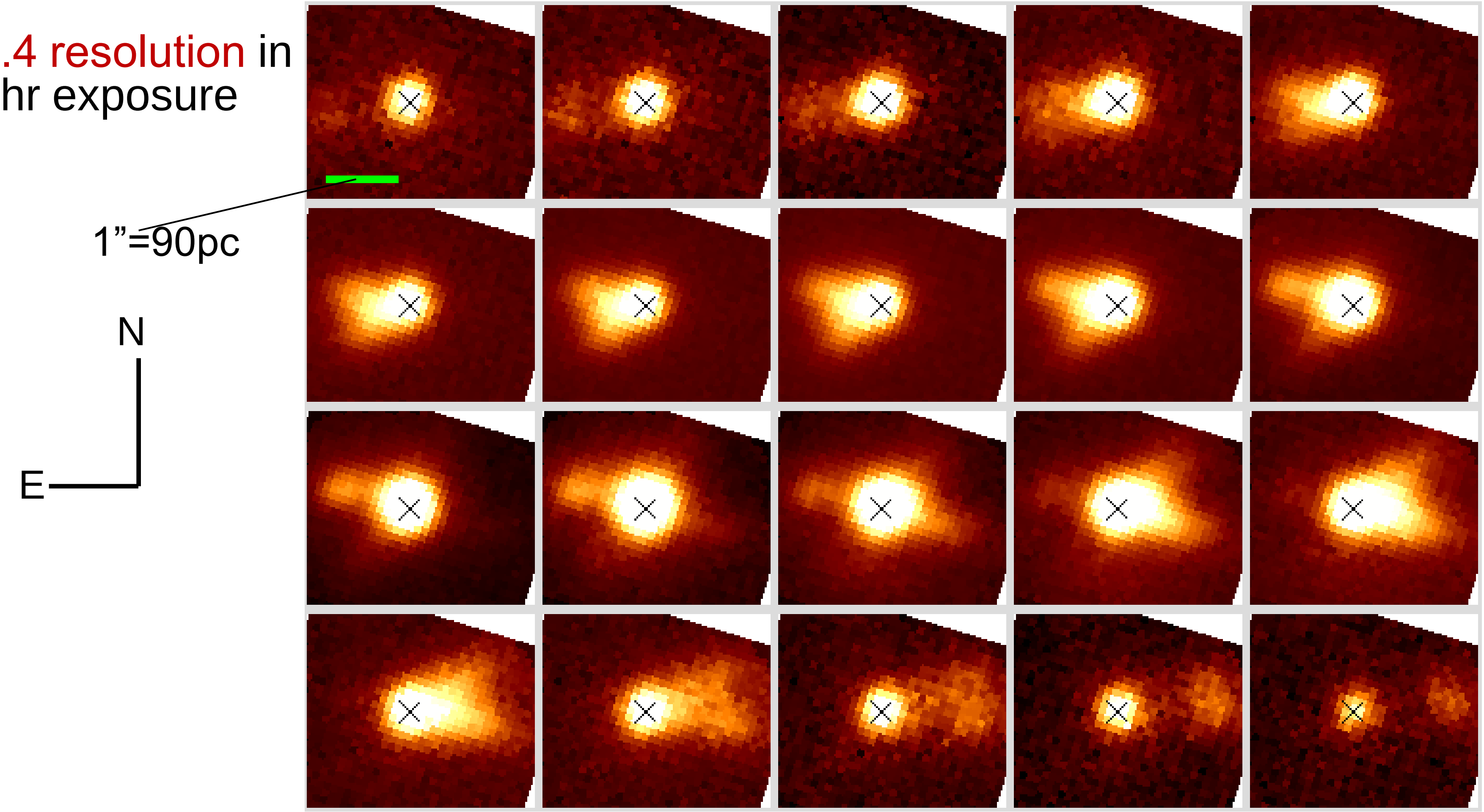

Velocity channel maps of the [OIII]λ5007 line for every 1.7 A, which corresponds to 102 km s^{-1}. The wavelength ranges from 5012.5 (*top left*) to 5044.8 A (*bottom right*). The intensity scale among the channels is arbitrary. The cross denotes the location of the line-free continuum peak.

Structures in bipolar outflow

The opening angle of the outflow decreases with velocity shift from the systemic velocity both in bluer and redder velocity channels.

-→ explained only if the outflow has intrinsically higher-velocity components inside, i.e., in regions closer to the outflow axis.

At both sides of the bipolar outflow, the highest velocity components are detached from the nucleus.

-→ This gap can be explained by an acceleration of at least a part of the flow or the surrounding matter, or by bow shocks that may be produced by even higher velocity outflow components that are not yet detected.

Bipolar outflow & radio jets

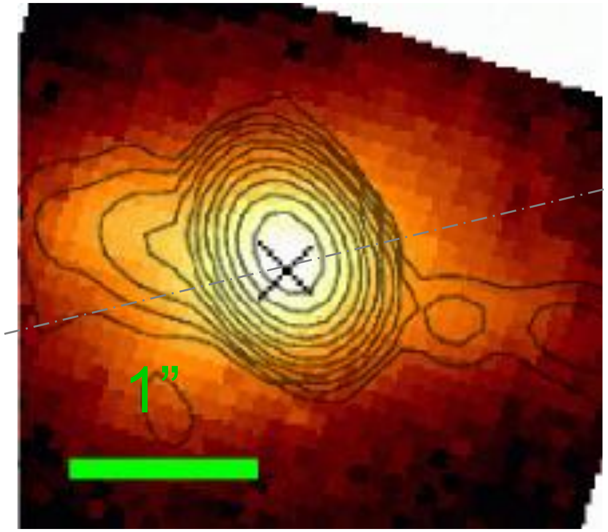

Comparison of [OIII]λ5007 line emission (color) ridges with MERLIN 1.4 GHz contours (Kadler et al. 2004)

5002.3 A 5068.6 A

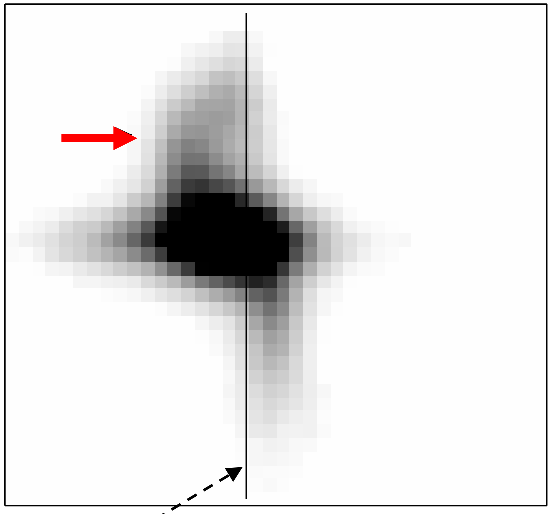

systemic velocity

Abrupt change in the velocity field

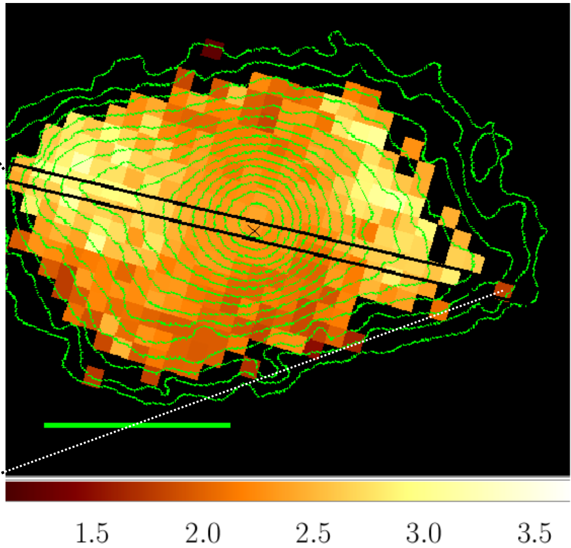

Spatial distribution of [OIII]λ5007/Hβ line ratio (color), with [OIII]λ5007 intensity contours

Strong [OIII] emission ridges along the edges of the outflow.

[left] closely related with the 1"-scale radio jet-counterjet structure.

[middle] abrupt change in the velocity field of the ionized gas.

[right] large [OIII] /Hβ flux ratio explained by shocks (~100km s^{-1}).

-→Strong interaction of the jets (+ some ridge components) with ISM.

Summary (NGC 1052)

High spatial resolution IFS of "prototypical" LINER NGC 1052

→Young (~10^5yr) outflow from AGN

Structures in outflow

Intrinsic velocity dependence on angle from outflow axis.

Acceleration?

or Bow shock by unseen high velocity component?

Relation with radio jets.

Integral field spectroscopy of the quadruply lensed quasar 1RXS J1131-1231: new light on lens substructures

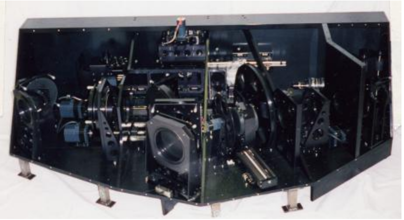

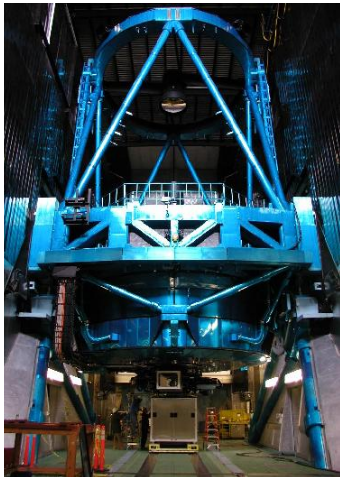

1. Macro/milli-lens
2. Microlens
3. Summary

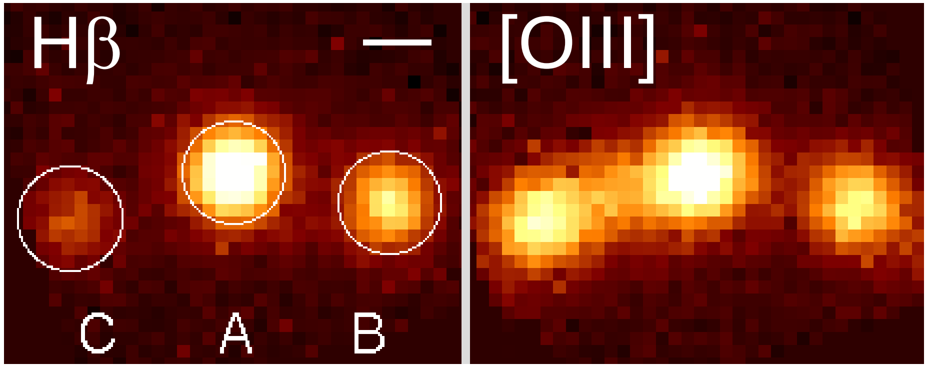

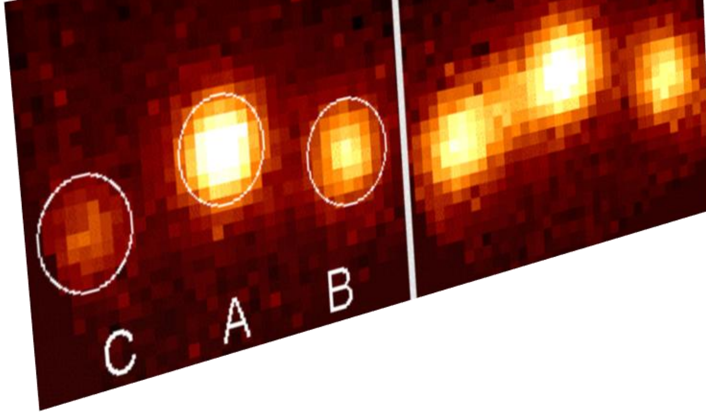

Point: 1RXS J1131-1231

using gravitational lensing, investigate both of **matter distribution in lens galaxy** and **internal structures in lensed quasar**

Three “kinds” of gravitational lenses

Macrolens (~$10^{12}M_\odot$)

Smooth potential of the whole lens galaxy.

Determines rough structure, such as lensed image positions.

[anomalous continuum flux ratios among quasar images in 1RXS J1131-1231]

Millilens (~$10^{8}M_\odot$)

CDM clumps expected in the lens galaxy halo.

Microlens (~$10^{0}M_\odot$)

each ~stellar mass object in the lens galaxy.

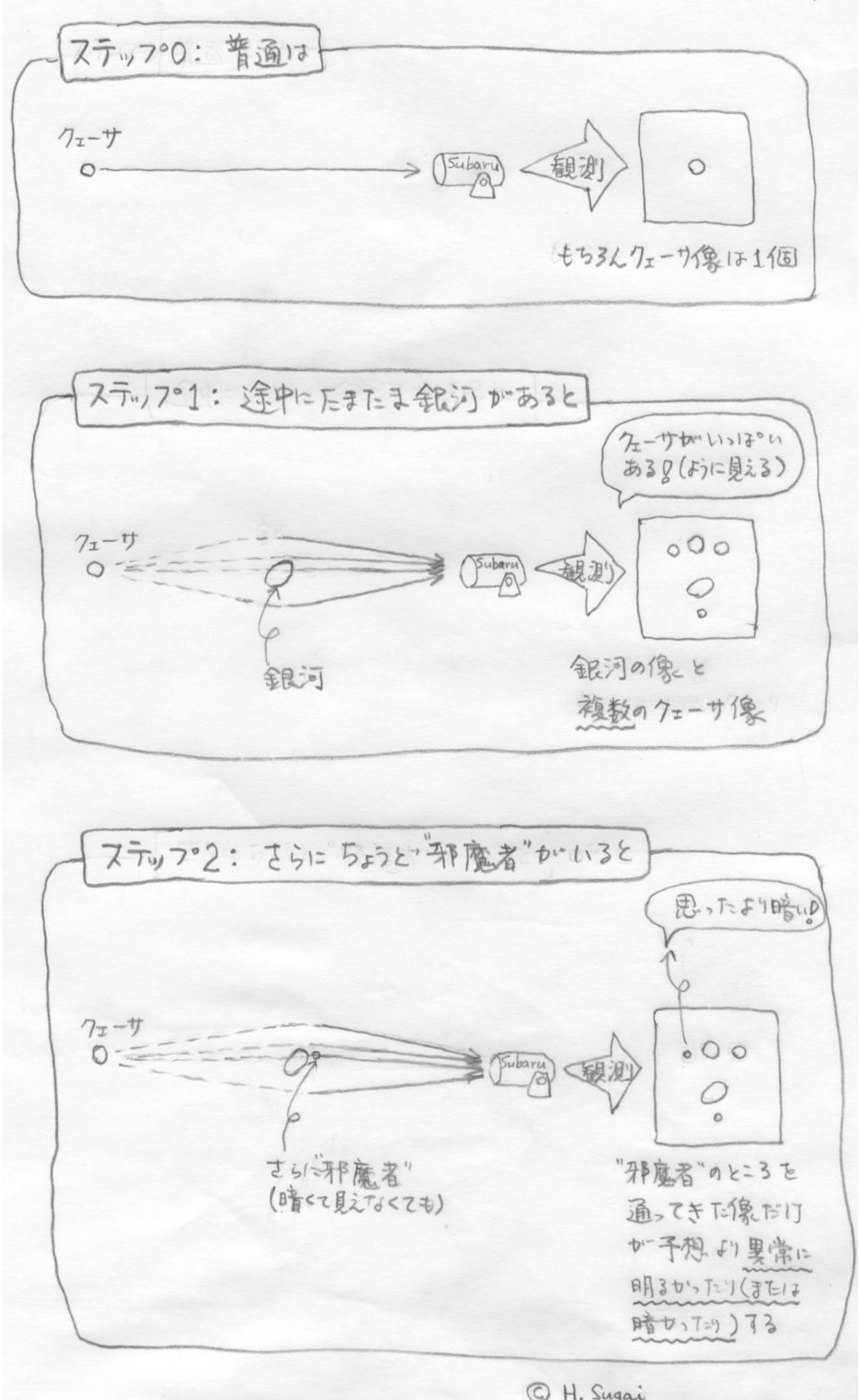

sorry, only in Japanese

Section 1

(Macro&)Milli-lens

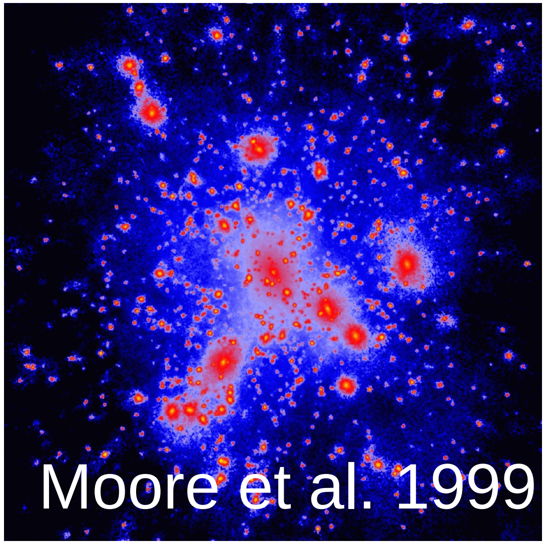

Investigating the existence of millilens by using Narrow line flux ratios among quasar images

When the Einstein radius ($\propto M_E^{1/2}$) is fixed,

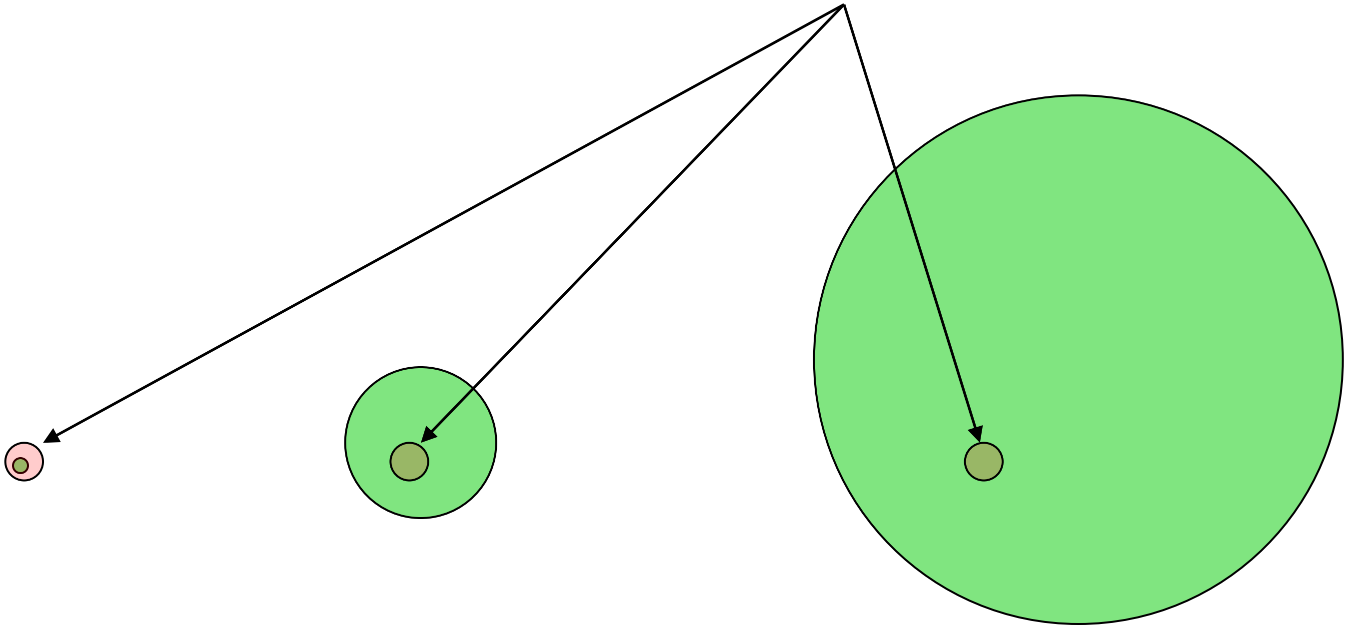

lensing effects on green-colored regions are

larger smaller

Micro/milli-lens mass & Emission line region size

This work

	Narrow line region 10^2pc ~$1.4\text{x}10^{-2}$ ”	Broad line region $10^{-1\sim-2}$pc ~$1.4\text{x}10^{-5\sim-6}$ ”
Microlens (star~$1M_{\odot}$ θ_E~$2.4\text{x}10^{-6}$ ”)	Not affected	Affected
Millilens (CDM subhalo ~$10^8M_{\odot}$ θ_E~$2.4\text{x}10^{-2}$ ”))	Affected	Affected

Observations

Kyoto 3DII IFS mode (37x37 lenslet array)
+ Subaru 8.2m telescope

Spatial sampling = 0”.096 lenslet^{-1}; FOV~3”.6 x 2”.8
Spatial resolution = 0”.5-0”.6

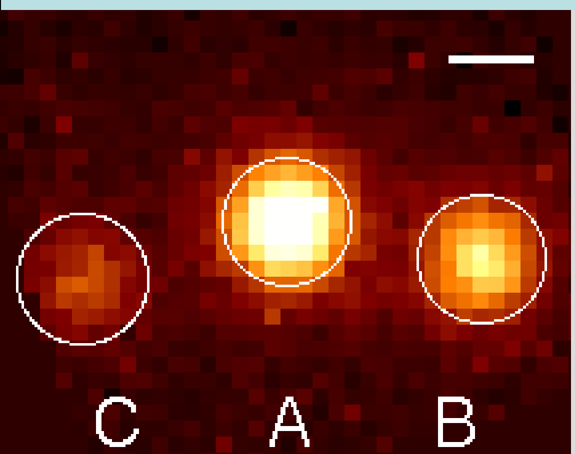

Hβ(broad line)

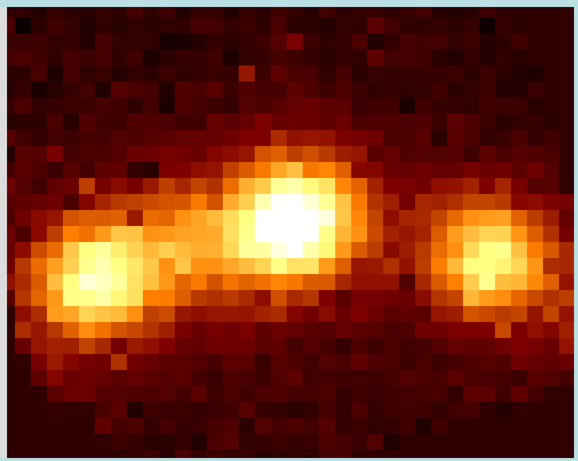

[OIII](narrow line)

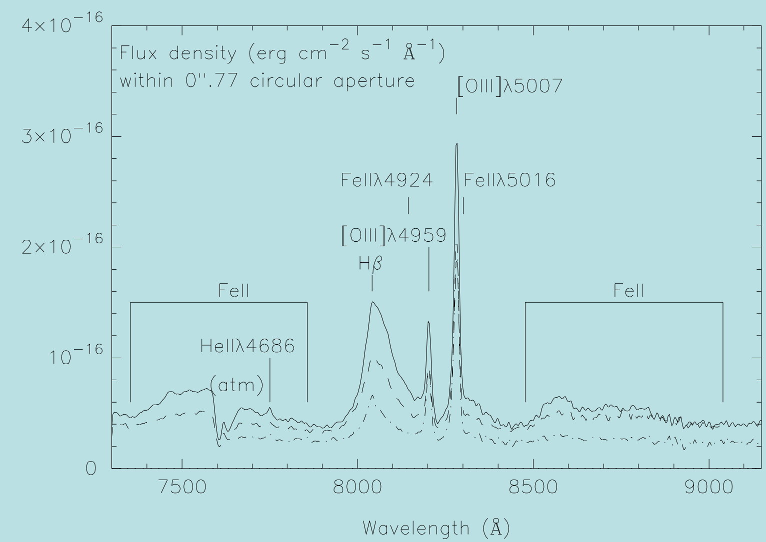

White bar = 0”.5 = 2.2kpc at z_{Lens}=0.295. z_S=0.658.
The faintest image D is out of FOV.

[OIII] ratios are consistent with macrolens model !

(As for C/B, contribution from extended emission between A & C.)

TABLE 1

RELATIVE FLUX RATIOS AMONG QUASAR IMAGES A, B, AND C

	Line[a]	A	B	C
Obs.	[O III]	$1.63^{+0.04}_{-0.02}$	1.00	$1.19^{+0.03}_{-0.12}$
	Hβ (broad)	$1.74^{+0.07}_{-0.12}$	1.00	$0.46^{+0.02}_{-0.03}$
Macrolens models	SIEx+[b]	1.66	1.00	0.91
	SISx[c]	1.75	1.00	1.00
	SISx[d]	1.70	1.00	0.96

Accurate flux ratio measurements.
image separation ~1”

Conclusion[1.1] Millilens

Mass of any substructures along the line of sight

(quasar images A, B, C)

$M_E < 10^5 M_\odot$

Conclusion[1.2] Macrolens

Resolging Structure of Narrow line region(asymmetry)

Without magnification,
~100pc =14milliarcsec

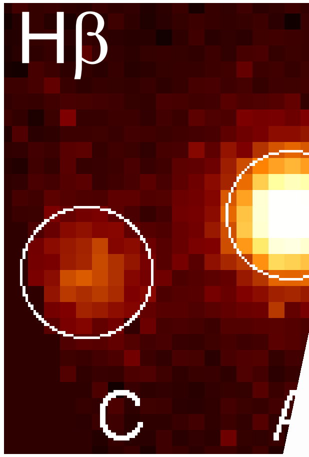

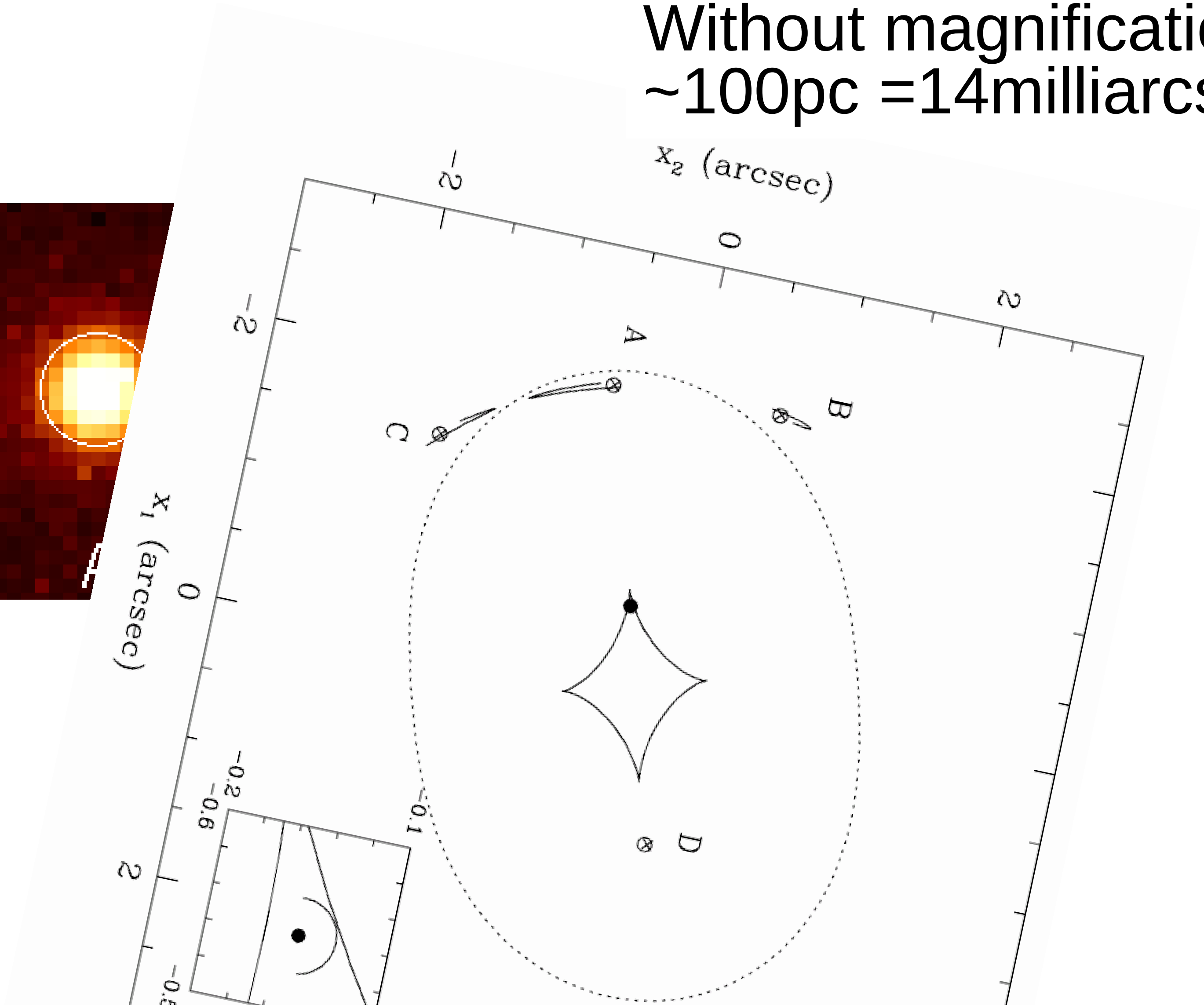

Section 2

Microlens

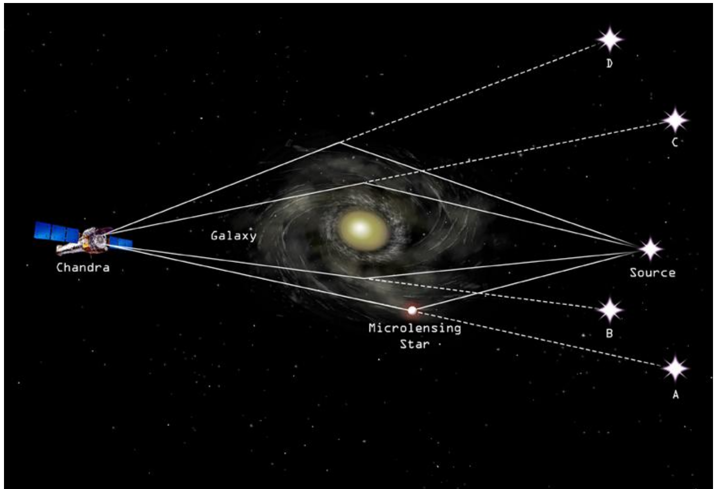

Credit: NASA/CXC/M.Weiss

Hβ: A/B ratio is consistent with macrolens model.

C/B ratio is inconsistent !

→ Microlens

TABLE 1

Relative Flux Ratios among Quasar Images A, B, and C

	Line[a]	A	B	C
Obs.	[O III]	$1.63^{+0.04}_{-0.02}$	1.00	$1.19^{+0.03}_{-0.12}$
	Hβ (broad)	$1.74^{+0.07}_{-0.12}$	1.00	$0.46^{+0.02}_{-0.03}$
Macro lens model	SIEx+[b]	1.66	1.00	0.91
	SISx[c]	1.75	1.00	1.00
	SISx[d]	1.70	1.00	0.96

Conclusion[2.1] Microlens

Quasar image C is demagnified by microlensing.

Conclusion[2.2] Microlens

“Resoving” structure of broad line region

The A/B ratio of Hβ(broad line) is consistent with macrolens model.

But line profiles differ between A & B.

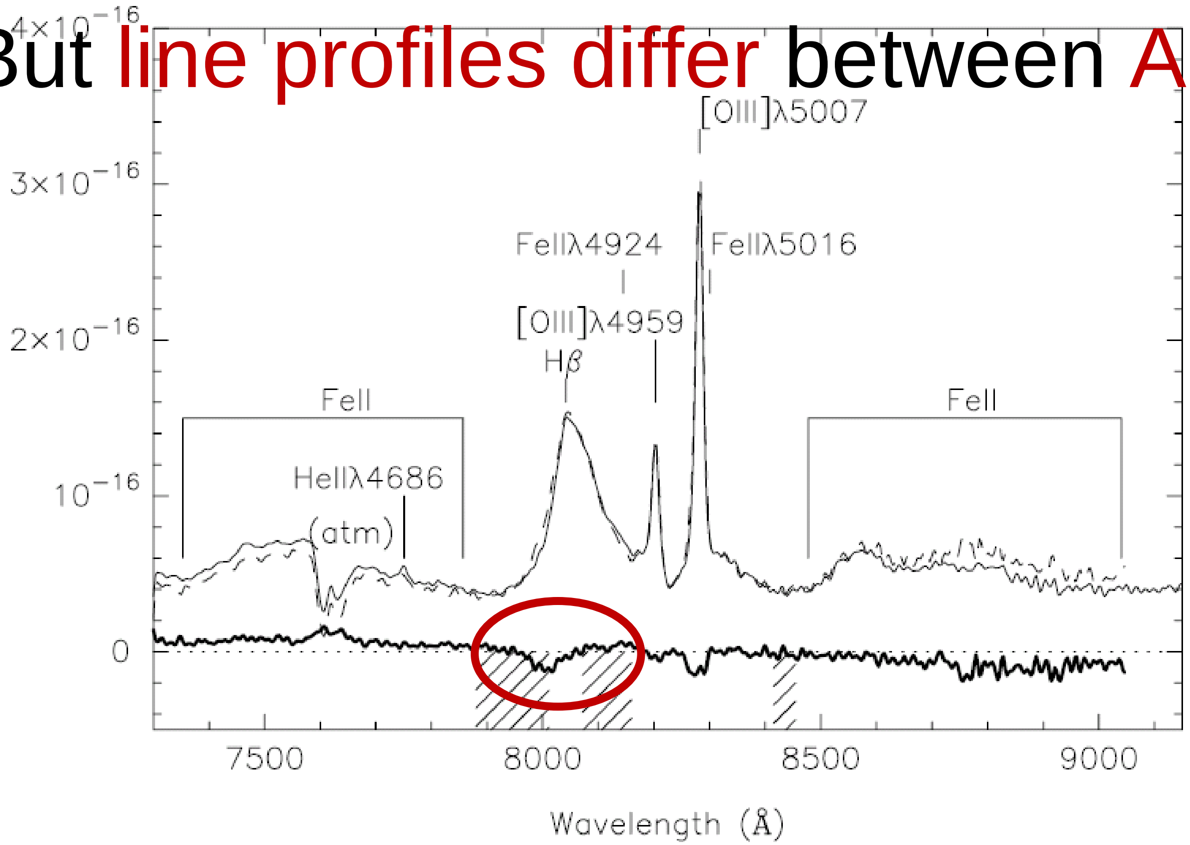

Comparison between image A & 1.74 x image B

“Resolving” structure of quasar broad line region with microlens

Line profile depends on which part is microlensed.

If gas is rotating,

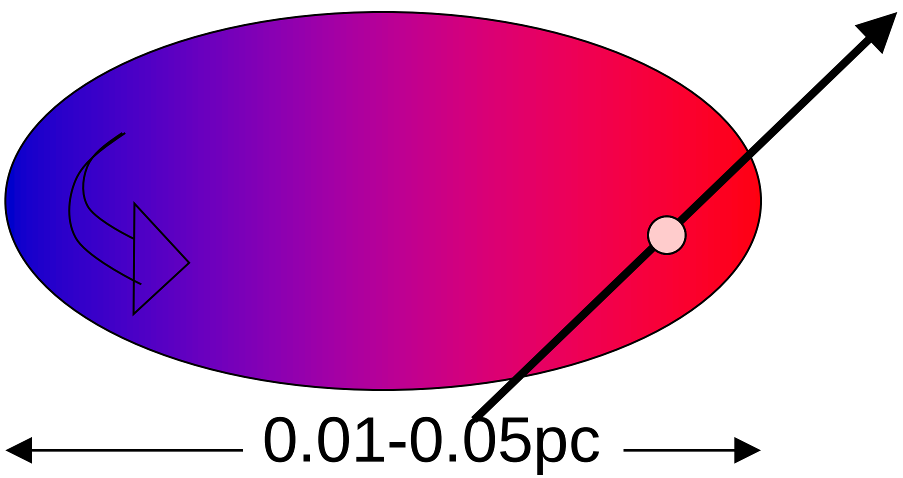

line profile will change when a microlens passes through.

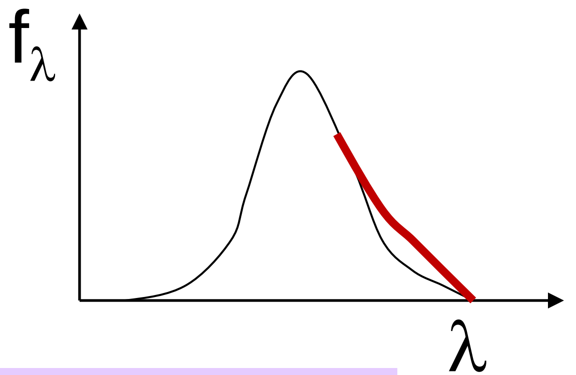

Better “resolution” than ~1μarcsec

Summary (1RXS J1131-1231)

Mass of any substructures along the line of sight $M_E<10^5 M_{\odot}$

Resolving the structure of quasar narrow line region (with macrolensing)

Microlenses for quasar broad line region

For quasar images C & (partially) A.

Resolving broad line region for image A.

Summary of this talk

IFS mode of Kyoto 3DII

Optimized for high spatial resolution
with ~0''.1 sampling

NGC 1052

AGN outflow structures

1RXS J1131-1231

Mass distribution in lens galaxy &
Structure of line emission regions in quasar